



Electromagnetic Simulations of Wide Angle and Polarization Insensitive Broadband Radar Absorbing Structure

*M. H. Ali*¹ and **M. B. Abdullahi*^{1,2}

¹Department of Physics, Bayero University Kano Nigeria

²Department of Physics, Usmanu Danfodiyo University Sokoto Nigeria

*Corresponding author: mhali.phy@buk.edu.ng, *abdullahi.bello@udusok.edu.ng

Article Info

Received 16 July 2020

Revised 02 Feb. 2021

Accepted 05 Feb. 2021

Available online 01 March. 2021

Keywords:

Keywords: Polarization, Radar Absorbing Structure, Simulation, Stealth, Wide-Angle.



<https://doi.org/10.37933/nipes/3.1.2021.1>

<https://nipesjournals.org.ng>
© 2021 NIPES Pub. All rights reserved.

Abstract

In this paper, we present the design and simulation of a wide-angle and polarization-insensitive broadband radar absorbing structure based on a lossy composite. The simulation was carried out in the COMSOL Multiphysics environment and the unit-cell of the design is composed of a three-layer structured assembly placed over a copper ground plane. The polarization and incident angle dependency of the designed absorber have been simulated. Also, its absorption behaviour was theoretically evaluated to validate the simulation result. The simulation result under normal incidence shows reflectivity below -10dB (over 90% absorption) in a broad frequency range from 5.1–18GHz. The simulation result was correlated with the calculated result and the results were found to be consistent with one another. Broadband absorption performance is stable for up to 30° incident angles in both the transverse electric (TE) and transverse magnetic (TM) polarization and insignificantly changes at 45°. Simulated reflectivity curves when polarization angles are varied from 0° to 60° under normal incidence are observed to overlapped, indicating that the proposed structure absorption level is indifferent to polarization directions. Therefore, the proposed radar absorbing structure can be suggested for potential applications in stealth and electromagnetic interference shielding.

1. Introduction

Radar absorbing materials (RAM) or coatings had been used in recent times to effectively absorb or reduce unwanted electromagnetic waves, thus are popularly used in the reduction of radar cross-section of various objects. Therefore, survival and infiltration abilities of military hardware used in modern warfare can be improved significantly when radar absorbing materials/coatings are used to minimize its radar cross-section [1]–[4]. Moreover, research interest in the development of radar absorbing materials is ever increasing due to the massive demand for effectively thin and lightweight broadband absorbing material as a result of advancement in radar detection technology [5]. Generally, radar absorbers can be classified as conventional material-based absorbers or structure-based absorbers where the latter received the most attention recently by using metamaterials (MM) and frequency selective surfaces (FSS) [6]. Structure-based absorbers can be ultra-thin [7], [8], as

well as exhibiting strong absorption over different frequency bands [9]–[11], making them as suitable candidates for stealth technology application [12].

Artificially engineered subwavelength composite structure commonly known as metamaterial had been extensively studied and deployed for several applications in acoustics and electromagnetic fields [13]–[18]. Landy et al.'s work on perfect metamaterial absorbers [19] stimulate research devotion on metamaterial absorbers (MMAs) and numerous designs have since been put forward, covering almost the entire electromagnetic spectrum spanning from microwaves [20], [21] through THz [22], [23] to the optical range [24]. The narrow bandwidth features of these MMAs, limit their practical applications where broadband absorption is paramount. For operational bandwidth enhancement, magnetic substrates had been adopted in many reports [4], [25]–[28] to replace the typical dielectric substrates employed in the design of these MMAs. However, the persistent challenge in MMAs design is to obtain simultaneously polarization independence, wide-angle of incidence, and wideband absorption behaviour. Thus, a new approach to overcoming this major challenge becomes particularly imperative.

To this end, we present a simulation-based radar absorbing structure (RAS) that demonstrates polarization insensitivity, wide-angle of incidence stability, and thin thickness in addition to its wideband absorption capability. The material used in the design is a spherical carbonyl iron powder/multiwalled carbon nanotube/silicon rubber (SCIP/MWCNT/SR) lossy composite developed by Huang et al. [29]. The power loss density simulation results indicated strong absorption taking place at the bottom layer of the structure for low frequencies, while for high frequencies it is at the surface layer and edges of the remaining layers. Calculated reflectivity of the presented RAS is in excellent accord with the simulated result of TE polarized radar wave under normal incidence.

2. Methodology

For validation purposes, a metamaterial absorber which was numerically and experimentally realized by Huang et al. [29] using CST Microwave Studio solver, was repeated on COMSOL Multiphysics solver used in this work. Focusing on 2-18 GHz band only, simulation results of flexible thin broadband microwave absorber based on a pyramidal periodic structure of lossy composite [29] is represented in Figure 1 alongside simulated results of the repeated metamaterial absorber using COMSOL Multiphysics. The simulation results are in close agreement in both shape and peaks as could be seen in Figure 1. This is a confirmation of the precision, reliability, and accuracy of the COMSOL Multiphysics numerical solver used in the present work.

To investigate the absorption properties of the proposed RAS, numerical simulations and optimization have been carried out by using the finite element method (FEM) based COMSOL Multiphysics solver. The electromagnetic parameters of the lossy composite as prepared and measured by [29] are imported into the simulation software to define the frequency-dependent material properties using an interpolation tool. Perfect magnetic conductor (PMC) and perfect electric conductor (PEC) boundary conditions are respectively applied along x and y axes to replicate an infinite array of the proposed RAS. The periodic port is used to supply incident plane-polarized electromagnetic waves along the z -axis plane. Impedance boundary condition (IBC) which treats any material behind the boundary as being infinitely large is chosen for the ground plane. Physics-controlled meshing is used in the simulation while the output of the simulation software is the scattering parameters (s – parameters). Maximum mesh element size was set at one-tenth of the minimum wavelength ($\frac{1}{10} \lambda_{min}$) of the input wave.

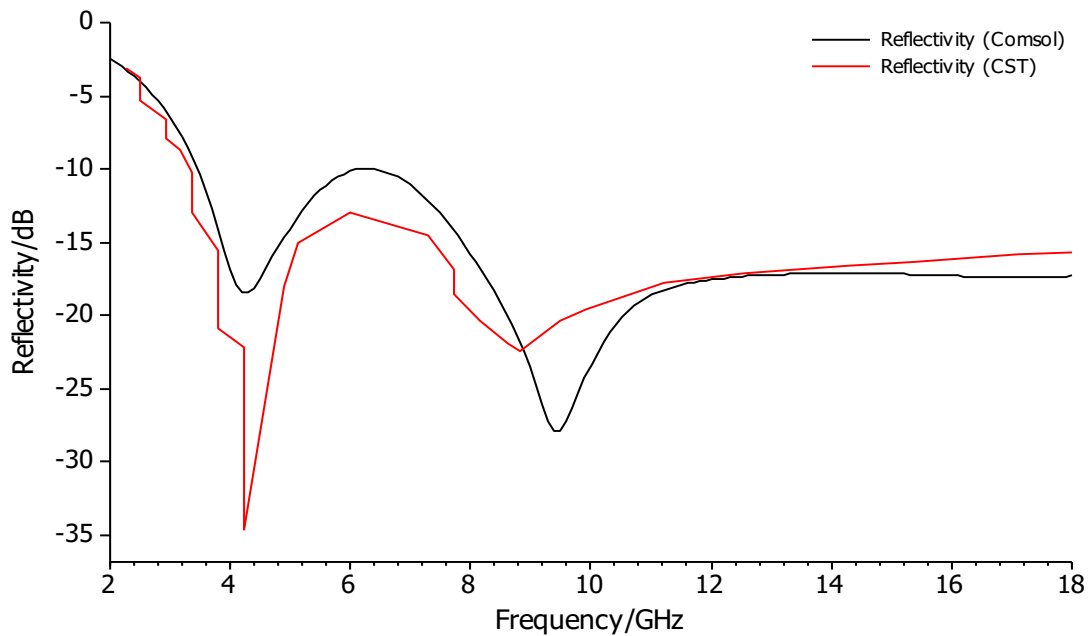


Figure 1: Simulated Reflectivity Plots for Comsol Multiphysics Software Validation

For the structure design, the basic idea is that the broadband absorption could be achieved by using the structured multilayer magnetic composite based designs [27], [30]. The optimized geometric structure of a single unit cell of the proposed broadband RAS is shown in Figure 2. It consists of three layers of the SCIP/MWCNT/SR lossy composite with a copper plate ground plane. The surface layer is cross-shaped, the middle layer is block shape structured and the bottom layer is considered as a conventional single slab absorber. The geometric dimensions of the RAS unit cell are optimized to ensure minimized reflectivity in the working frequency band. The thickness of the copper plate ground plane is designed to be greater than its skin depth for the radar frequency range, to prevent transmission of radiation.

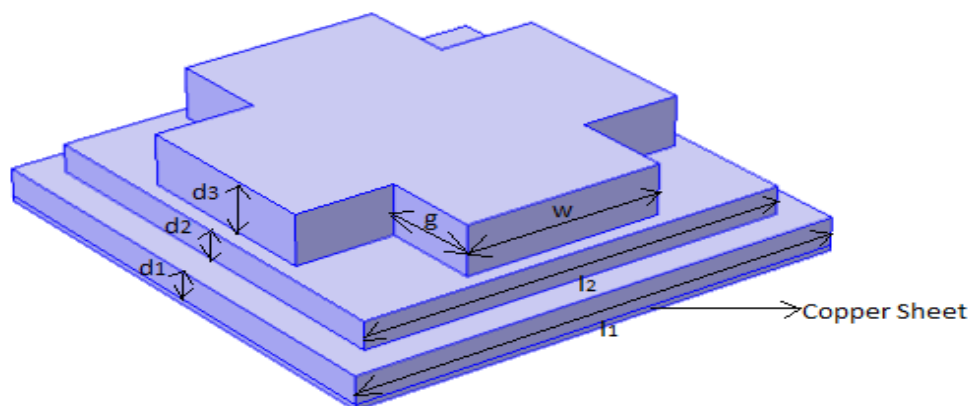


Figure 2: Designed Unit Cell Structure of the Proposed Radar Absorbing Structure, $l_1 = 15.0mm$, $l_2 = 13.0mm$, $w = 6.0mm$, $g = 3.0mm$, $d_1 = 1.0mm$, $d_2 = 1.0mm$, $d_3 = 1.8mm$.

As a three-layer structure, effective electromagnetic parameters of the surface and middle layers were calculated using the strong fluctuation theory of honeycomb-structured surfaces given in Equation (1) [31]. Based on Chew's model [32], $\tilde{R}_{i,i+1}$ in Equation (2) is evaluated recursively to

calculate the reflectivity of the broadband RAS. The calculated reflectivity is then compared with the simulated reflectivity to validate the performance of the designed RAS.

$$\varepsilon_{eff} = \frac{1}{2}[(1 - 2g)(1 - \varepsilon_r) + \sqrt{(1 - 2g)^2(1 - \varepsilon_r)^2 + 4\varepsilon_r}] \quad (1)$$

here, ε_{eff} is the effective permittivity, g is the volume ratio of the solid part in a layer, and ε_r is the permittivity of the solid. Effective permeability μ_{eff} can be obtained by replacing ε_r with μ_r in Equation (1).

$$\tilde{R}_{i,i+1} = \frac{R_{i,i+1} + \tilde{R}_{i+1,i+2} e^{-j2k_{i+1,z} d_{i+1}}}{1 + R_{i,i+1} \tilde{R}_{i+1,i+2} e^{-j2k_{i+1,z} d_{i+1}}} \quad (2)$$

where $R_{i,i+1} = \frac{\mu_{i+1}k_{i,z} - \mu_i k_{i+1,z}}{\mu_{i+1}k_{i,z} + \mu_i k_{i+1,z}}$ for TE wave, $R_{i,i+1} = \frac{\varepsilon_{i+1}k_{i,z} - \varepsilon_i k_{i+1,z}}{\varepsilon_{i+1}k_{i,z} + \varepsilon_i k_{i+1,z}}$ for TM wave,

$k_{i,z} = \omega\sqrt{\mu_i \varepsilon_i - \mu_0 \varepsilon_0 \sin^2 \theta}$, ε_i and μ_i are the complex permittivity and permeability respectively for the i^{th} layer, θ_i is the angle of transmission in the i^{th} layer while d_i is the i^{th} layer thickness.

3. Results and Discussion

The reflectivity spectrum of the model absorber was first studied under normal incidence for transverse electric (TE) polarization. We present the simulated and calculated reflectivity of the RAS under normal incident waves in Figure 3, which is based on the FEM method-based solver and Chew's model, respectively. It can be seen that; the calculated reflectivity is in good agreement with the simulation result which confirms the reliability of our simulation results and the validity of our design. The bandwidth of below -10dB reflectivity is 14.6 GHz (3.4-18 GHz) for the simulated and 15.0 GHz (3.0-18 GHz) for the calculated.

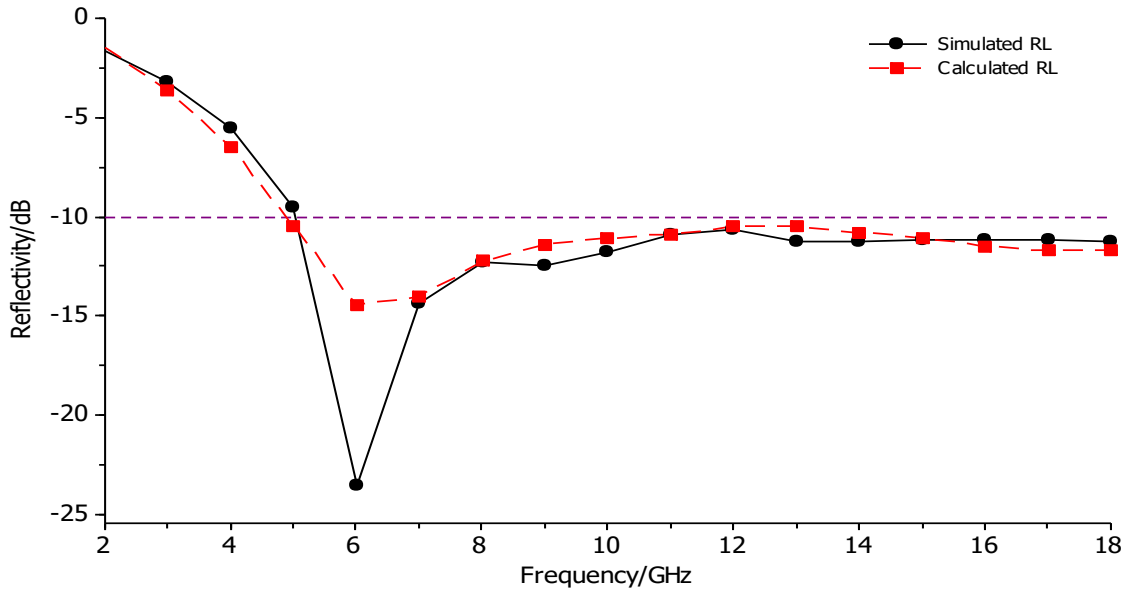


Figure 3: Simulated and Calculated Reflectivity Plots for TE Polarization at Normal Incidence

It is an important requirement for practical applications of radar absorbers to establish a stabilized excellent electromagnetic wave absorption in a wide incident angle range for both TE and TM polarization modes. Figure 4 indicates the simulated reflectivity of the proposed broadband RAS when the incident angle of TE polarization varies from 0° to 60° at 15° intervals. That of TM polarization is shown in Figure 5, where the incident angle is changed from 0° to 45° at 15° intervals. It can be seen that the broadband absorption performance is kept stable up to 30° incident angles for both the TE and TM polarizations. When the incident angle is increased to 60° and 45° for TE and TM polarizations respectively, the absorption bandwidth becomes a little narrower. For the TE

polarization as shown in Figure 4, the reflectivity bandwidth satisfying the below -10 dB reflectivity shifted to lower frequencies as incident angle increases. While the reflectivity bandwidth is 11.4 GHz at 45° (4.5 to 15.9 GHz), it's 10.8 GHz at 60° (4.2 to 15 GHz). Dual-band reflectivity is observed in the 2-18GHz radar range for the TM polarization when the incident angle is 45° as shown in Fig. 5 and the combined bandwidth is 6.5 GHz. To sum it up, greater than 80% absorptivity (-7dB reflectivity) is obtained for both TE and TM polarization in the 0° to 60° incident angle range. Therefore, it can be concluded that the designed RAS can work over a wide incident angle for both TE and TM polarizations.

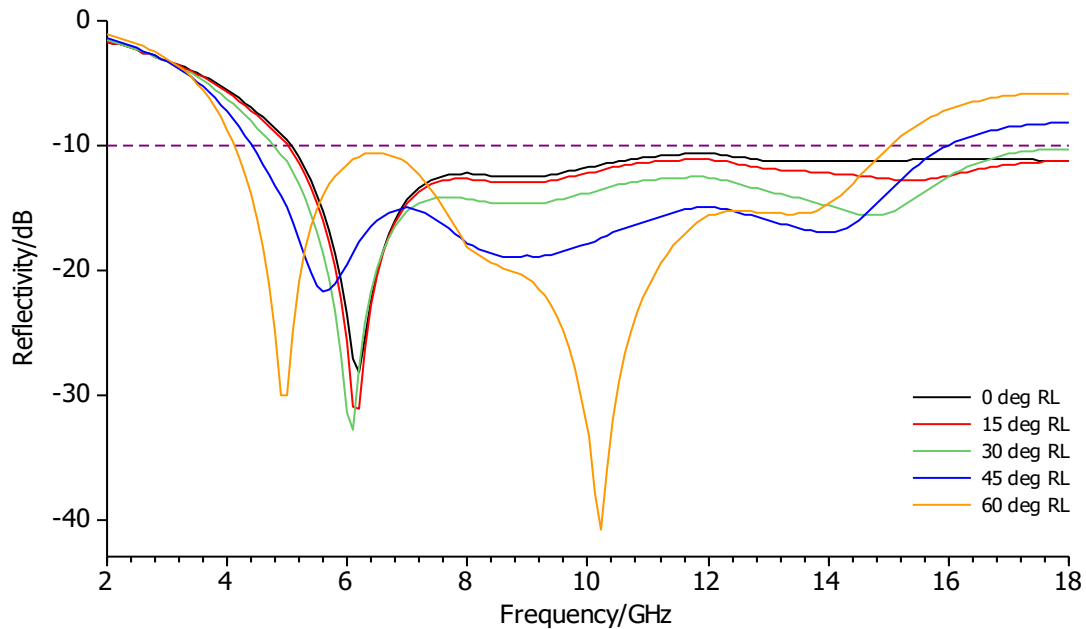


Figure 4: Simulated Reflectivity Plots for TE Polarization at Normal and Oblique Incidence

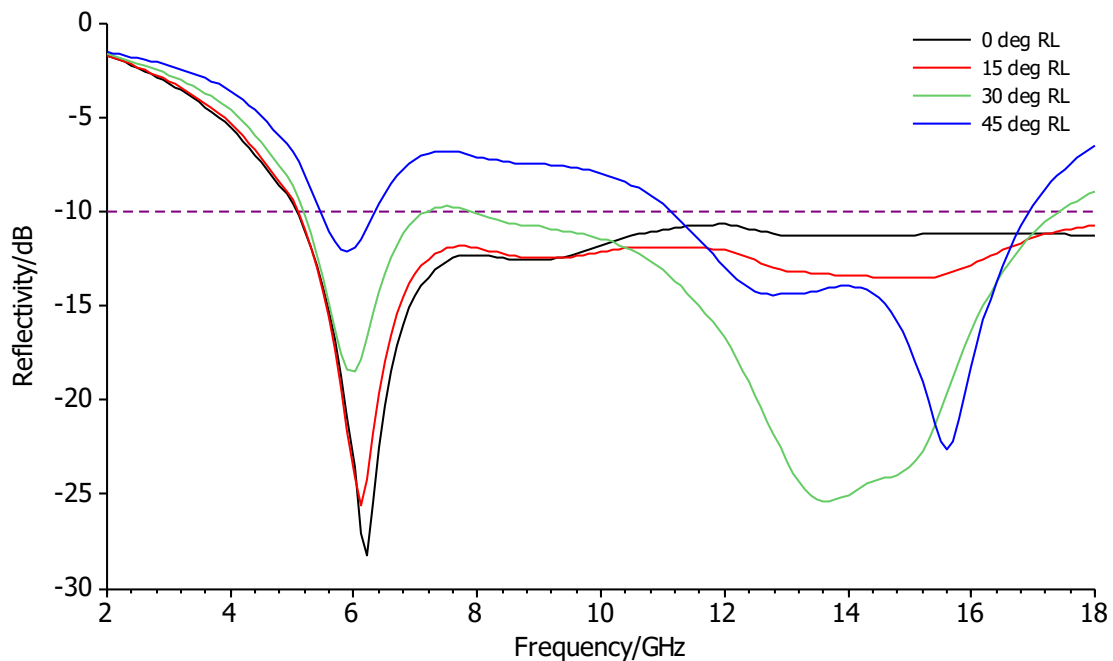


Figure 5: Simulated Reflectivity Plots for TM Polarization at Normal and Oblique Incidence

In Figure 6, simulated reflectivity curves when polarization angles are varied from 0^0 to 60^0 under normal incidence are observed to overlapped, indicating that the proposed RAS absorption level is indifferent to polarization directions. Under oblique incidence as shown in Figure 7, the reflectivity curves are closely packed and approximately maintaining the same bandwidth falling below -10dB reflectivity reference level. Hence, our design structure can be described as a polarization-insensitive absorber.

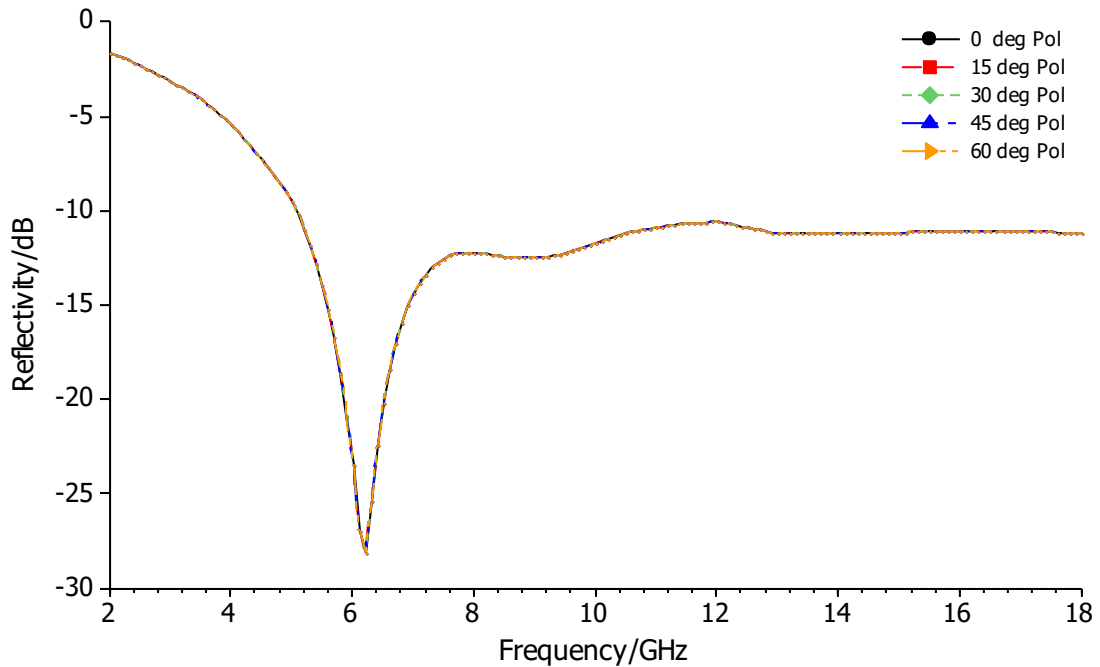


Figure 6: Simulated Reflectivity Plots for different Polarization angles at Normal Incidence

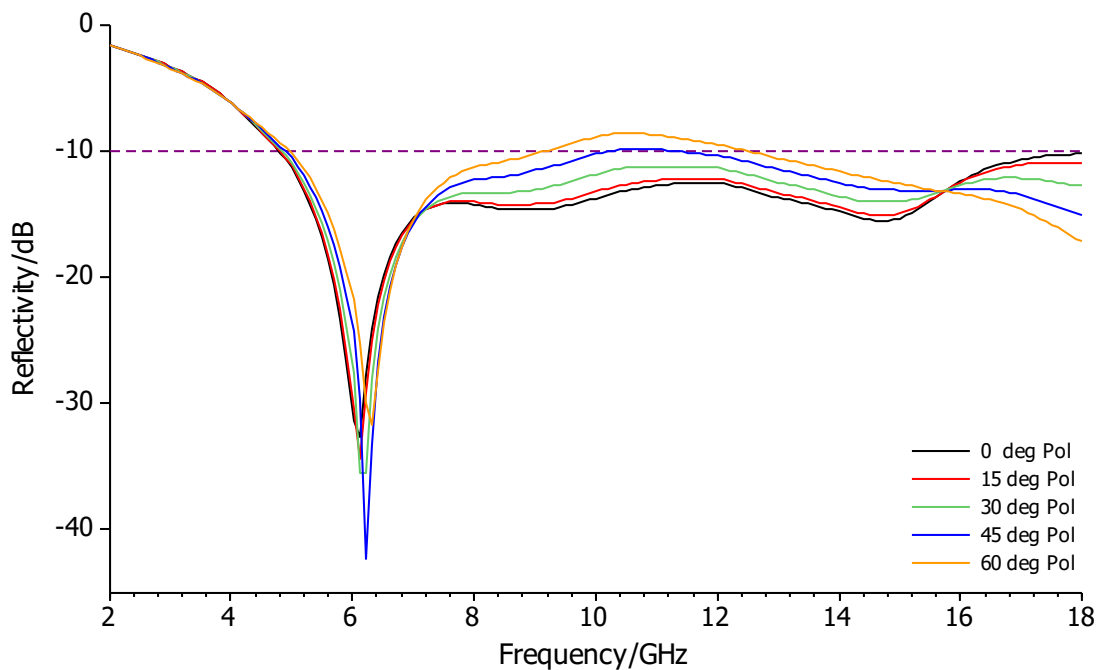
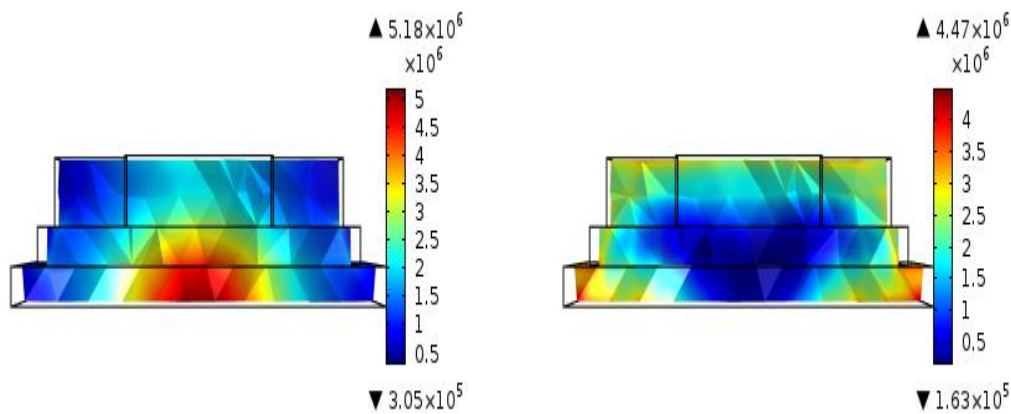


Figure 7: Simulated Reflectivity Plots for different Polarization angles at 30^0 Incidence

To better understand the physical mechanism of the observed broadband absorption of the proposed RAS, the power loss density of the unit-cell structure has been simulated as shown in Figure 8. Simulated power loss density at 6.2 GHz peak reflectivity in Figure 8a is observed to be concentrated at the central position of the bottom layer and aligned with the surface layer spot. This could be primarily ascribed to excellent impedance matching provided by the surface layer, hence allowing lower frequencies (2-8 GHz) transmission to the bottom layer for efficient absorption. Magnetic based composites, such as the SCIP/MWCNT/SR composites employed in our design is known to weakly absorb lower frequencies [33]. At 13.5 GHz revealed in Figure 8b, the main loss occurs at the surfaces and edges of the structure. This indicates that at high frequencies (8-18 GHz), the composite material can effectively absorb these frequencies at relatively thinner thickness. Furthermore, it can be also observed that the peak power loss density of $5.18 \times 10^6 \text{ Wm}^{-2}$ was obtained for the 6.2 GHz simulation, while $4.47 \times 10^6 \text{ Wm}^{-2}$ was recorded for the 13.5 GHz result. Therefore; the high reflectivity level of the broadband wide-angle and polarization-insensitive RAS of the present work can be achieved by structuring the composite material thereby enhancing its absorption capabilities at lower frequencies.



(a) (b)
Figure 8: Vertical Cross-Section of Power Loss Density Distribution at (a) 6.2 GHz and (b) 13.5 GHz for TE Polarization under Normal Incidence

To buttress the point that the structuring of the composite material enhances its absorption capabilities, we simulated an absorber designed from the same material and thickness and study its absorption performance for TE polarized wave under normal wave incidence. It is obvious from the curves in Figure 9 that the designed RAS outperformed its unstructured counterpart.

The performance of the proposed MMA is compared uniquely with that of Huang et al [29] SPS absorber. Though Huang and Co-authors established a broadband absorption in the 2-40 GHz, prepare, fabricate and introduce the composite material we used, we limited our effort within the reported 2-18 GHz frequency range considered in the measurements of the electromagnetic parameters of the composite material. In addition to the flexibility characteristics of the material for the RAS when experimentally realized, our work reports the performance of the absorber under oblique incidence and different polarization angle conditions. It was found to exhibit a wide-angle and polarization-insensitive characteristic. Furthermore, the bandwidth to thickness ratio is 11.39 which is very close to the 11.53 value obtained in [29], and it is only 3.8mm in thickness.

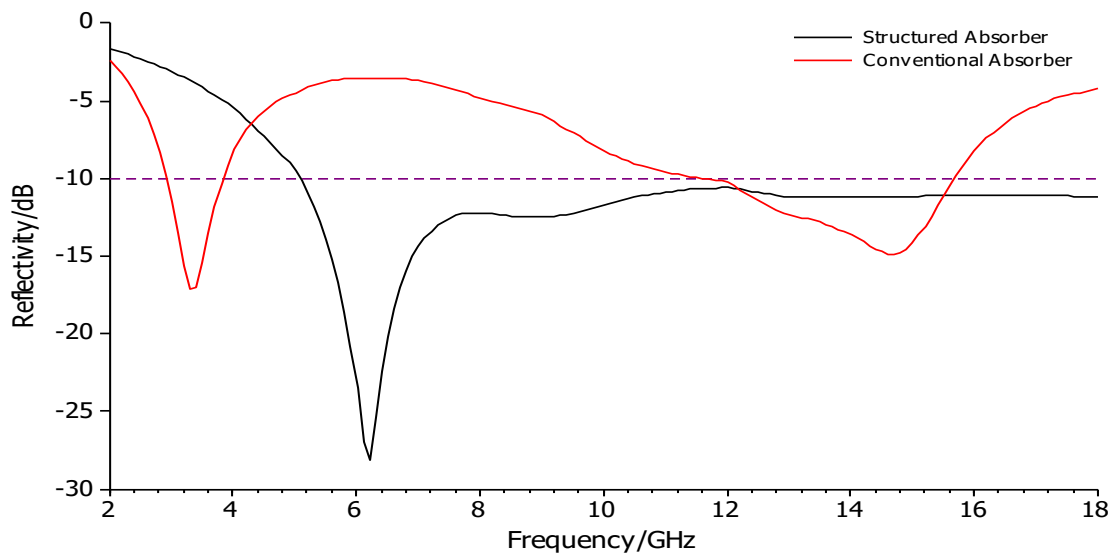


Figure 9: Simulated Reflectivity Plots of Structured and Unstructured Absorbers for TE Polarization at Normal Incidence

4. Conclusion

Based on lossy composite material, we present the electromagnetic simulation of a three-layer structured radar absorber that demonstrates broadband absorption, wide-angle of incidence stability, and polarization indifference behaviour. Electromagnetic power loss density simulation revealed that the bottom layer dominates absorption at lower frequencies, while the surface layer and edges of the remaining layers define the main power loss at high frequencies. Therefore, the proposed structure improves the absorption characteristics of the lossy composite employed in the design. The proposed RAS can be useful for experimental work and the potential applications of the current RAS in stealth technology, as well as electromagnetic interference suppression, emanates from its wide-angle, polarization independence, and wideband absorption characteristics.

References

- [1] Y. Pang, H. Cheng, Y. Zhou, Z. Li, and J. Wang, "Ultrathin and broadband high impedance surface absorbers based on metamaterial substrates," vol. 20, no. 11, pp. 12515–12520, 2012.
- [2] M. Chen, Y. Pei, and D. Fang, "Design, fabrication, and characterization of lightweight and broadband microwave absorbing structure reinforced by two dimensional composite lattice," pp. 75–80, 2012, doi: 10.1007/s00339-012-7002-7.
- [3] Y. Pinto, J. Sarrazin, A. Claire, and L. Xavier, "Design and measurement of a thin and light absorbing material for space applications Design and measurement of a thin and light absorbing material," no. May, 2014, doi: 10.1007/s00339-013-8097-1.
- [4] H. Xu, S. Bie, Y. Xu, W. Yuan, Q. Chen, and J. Jiang, "Broad bandwidth of thin composite radar absorbing structures embedded with frequency selective surfaces," *Compos. PART A*, 2015, doi: 10.1016/j.compositesa.2015.10.019.
- [5] W. Li, L. Lin, C. Li, Y. Wang, and J. Zhang, "Radar absorbing combinatorial metamaterial based on silicon carbide / carbon foam material embedded with split square ring metal," *Results Phys.*, vol. 12, no. August 2018, pp. 278–286, 2019, doi: 10.1016/j.rinp.2018.11.036.
- [6] and S. B. Yun He, Jianjun Jiang, Mi Chen, Shicai Li, Ling Miao, "Design of an adjustable polarization-independent and wideband electromagnetic absorber," *J. Appl. Phys.*, vol. 119, no. 10, 2016.
- [7] H. Li *et al.*, "Ultrathin multiband gigahertz metamaterial absorbers," vol. 110, no. 1, 2011, doi: 10.1063/1.3608246.
- [8] S. Li *et al.*, "Wideband , thin , and polarization-insensitive perfect absorber based the double octagonal rings metamaterials and lumped resistances Wideband , thin , and polarization-insensitive perfect absorber based the double octagonal rings metamaterials and lumped," *J. Appl. Phys.*, vol. 116, no. 4, 2014, doi: 10.1063/1.4891716.

- [9] C. Hu, Z. Zhao, X. Chen, and X. Luo, "Realizing near-perfect absorption at visible frequencies," *Opt. Express*, vol. 17, no. 13, pp. 11039–11044, 2009.
- [10] H. Tao *et al.*, "Highly flexible wide angle of incidence terahertz metamaterial absorber : Design , fabrication , and characterization," *Phys. Rev. B*, vol. 78, no. 4, pp. 2–5, 2008, doi: 10.1103/PhysRevB.78.241103.
- [11] G. Yang *et al.*, "Broadband polarization-insensitive absorber based on gradient structure metamaterial Broadband polarization-insensitive absorber based on gradient structure metamaterial," *J. Appl. Phys.*, vol. 115, no. 17, pp. 2013–2016, 2014, doi: 10.1063/1.4868090.
- [12] L. Zhang *et al.*, "A Broadband Radar Absorber Based on Perforated Magnetic Polymer Composites Embedded With FSS," *IEEE Trans. Magn.*, vol. 50, no. 5, 2014.
- [13] F. Ö. Alkurt, M. Bağmanç, and M. Karaaslan, "Design of a Dual Band Metamaterial Absorber for Wi-Fi Bands," in *AIP Conference Proceedings*, 2018, vol. 1935, pp. 1–5, doi: 10.1063/1.5025979.
- [14] Q. Chen, S. Bie, W. Yuan, Y. Xu, H. Xu, and J. Jiang, "Low frequency absorption properties of a thin metamaterial absorber with cross-array on the surface of a magnetic substrate," *J. Phys. D: Appl. Phys.*, vol. 49, p. 425102, 2016, doi: 10.1088/0022-3727/49/42/425102.
- [15] W. Chen, C. M. Bingham, K. M. Mak, N. W. Caira, and W. J. Padilla, "Extremely subwavelength planar magnetic metamaterials," vol. 201104, pp. 1–5, 2012, doi: 10.1103/PhysRevB.85.201104.
- [16] X. Huang, X. He, L. Guo, and Y. Yi, "Analysis of ultra-broadband metamaterial absorber based on simplified multi-reflection interference theory," *J. Opt.*, vol. 17, no. 5, p. 55101, 2015, doi: 10.1088/2040-8978/17/5/055101.
- [17] Y. Zhu, X. Fan, B. Liang, J. Cheng, and Y. Jing, "Ultrathin Acoustic Metasurface-Based Schroeder Diffuser," *Phys. Rev. X*, vol. 7, no. 2, pp. 1–11, 2017, doi: 10.1103/PhysRevX.7.021034.
- [18] Y. Liu *et al.*, "Fractal Acoustic Metamaterials with Subwavelength and Broadband Sound Insulation," *Shock Vib.*, vol. 2019, 2019.
- [19] N. I. Landy, S. Sajuyigbe, J. J. Mock, D. R. Smith, and W. J. Padilla, "Perfect metamaterial absorber," *Phys. Rev. Lett.*, vol. 100, no. 20, pp. 1–4, 2008, doi: 10.1103/PhysRevLett.100.207402.
- [20] W. Xu and S. Sonkusale, "Microwave diode switchable metamaterial reflector / absorber Microwave diode switchable metamaterial reflector / absorber," *Appl. Phys. Lett.*, vol. 103, no. 3, pp. 3–7, 2013, doi: 10.1063/1.4813750.
- [21] F. Ding, Y. Cui, X. Ge, Y. Jin, and S. He, "Ultra-Broadband Microwave Metamaterial Absorber," *Appl. Phys. Lett.*, vol. 100, no. 10, 2012, doi: 10.1063/1.3692178.
- [22] Q. Wen, H. Zhang, Y. Xie, Q. Yang, and Y. Liu, "Dual band terahertz metamaterial absorber : Design , fabrication , and characterization," *Appl. Phys. Lett.*, vol. 95, no. 24, 2009, doi: 10.1063/1.3276072.
- [23] J. Zhu, W. Sun, F. Ding, Q. He, and L. Zhou, "Ultra-broadband terahertz metamaterial absorber," *Appl. Phys. Lett.*, vol. 105, no. 2, 2014, doi: 10.1063/1.4890521.
- [24] J. Wang *et al.*, "Tunable broad-band perfect absorber by exciting of multiple plasmon resonances at optical frequency," *Opt. Express*, vol. 20, no. 14, pp. 14871–14878, 2012, doi: 10.1007/s00339-012-6936-0.25.
- [25] D. Wan, S. Bie, J. Zhou, H. Xu, Y. Xu, and J. Jiang, "A Thin and Broadband Microwave Absorber Based on Magnetic Sheets and Resistive FSS," *Prog. Electromagn. Res. C*, vol. 56, no. 2, pp. 93–100, 2015.
- [26] W. Yuan, Q. Chen, Y. Xu, H. Xu, S. Bie, and J. Jiang, "Broadband Microwave Absorption Properties of Ultrathin Composites containing Edge-split Square-loop FSS embedded in Magnetic Sheets," vol. 1225, no. c, pp. 2–5, 2016, doi: 10.1109/LAWP.2016.2572734.
- [27] Y. Xu, W. Yuan, S. Bie, H. Xu, Q. Chen, and J. Jiang, "Broadband microwave absorption property of a thin metamaterial containing patterned magnetic sheet," *J. Electromagn. Waves Appl.*, vol. 29, no. 18, pp. 2420–2427, 2015, doi: 10.1080/09205071.2015.1077751.
- [28] W. Li *et al.*, "Low frequency and broadband metamaterial absorber with cross arrays and a flaked iron powder magnetic composite Low frequency and broadband metamaterial absorber with cross arrays and a flaked iron powder magnetic composite," *AIP Adv.*, vol. 8, no. 1, pp. 015318–1 to 015318–9, 2018.
- [29] Y. Huang, X. Yuan, C. Wang, M. Chen, L. Tang, and D. Fang, "Flexible thin broadband microwave absorber based on a pyramidal periodic structure of lossy composite," *Opt. Lett.*, vol. 43, no. 12, pp. 2764–2767, 2018.
- [30] M. B. Abdullahi and M. H. Ali, "Design and Simulation of Cross-Block Structured Radar Absorbing Metamaterial Based on Carbonyl Iron Powder Composite," *Niger. J. Technol.*, vol. 38, no. 4, pp. 912–918, 2019.
- [31] D. Zhou, X. Huang, Z. Du, and Q. Wang, "Calculation and Analysis of the Effective Electromagnetic Parameters of Periodic Structural Radar Absorbing Material Using Simulation and Inversion Methods," vol. 52, no. October, pp. 57–66, 2016.
- [32] N. Dib, M. Asi, and A. Sabbah, "On the optimal design of multilayer microwave absorbers," *Prog. Electromagn. Res. C*, vol. 13, pp. 171–185, 2010, doi: 10.2528/PIERC10041310.
- [33] W. Li, T. Wu, W. Wang, J. Guan, and P. Zhai, "Integrating non-planar metamaterials with magnetic absorbing materials to yield ultra-broadband microwave hybrid absorbers," *Appl. Phys. Lett.*, vol. 104, no. 2, pp. 16–21, 2014, doi: 10.1063/1.4862262.